Basic Res Cardiol (2017) 112:57
DOI 10.1007/s00395-017-0646-x

ORIGINAL CONTRIBUTION

Methylglyoxal-derived advanced glycation end products contribute to negative cardiac remodeling and dysfunction post-myocardial infarction

Nick J. R. Blackburn[1,2] · Branka Vulesevic[1,2] · Brian McNeill[1] · Cagla Eren Cimenci[1,2] · Ali Ahmadi[1,2] · Mayte Gonzalez-Gomez[1,2] · Aleksandra Ostojic[1,2] · Zhiyuan Zhong[3] · Michael Brownlee[4] · Paul J. Beisswenger[5] · Ross W. Milne[6] · Erik J. Suuronen[1,2]

Received: 21 February 2017 / Accepted: 29 August 2017 / Published online: 1 September 2017

Abstract Advanced glycation end-products (AGEs) have been associated with poorer outcomes after myocardial infarction (MI), and linked with heart failure. Methylglyoxal (MG) is considered the most important AGE precursor, but its role in MI is unknown. In this study, we investigated the involvement of MG-derived AGEs (MG-AGEs) in MI using transgenic mice that over-express the MG-metabolizing enzyme glyoxalase-1 (GLO1). MI was induced in GLO1 mice and wild-type (WT) littermates. At 6 h post-MI, mass spectrometry revealed that MG-H1 (a principal MG-AGE) was increased in the hearts of WT mice, and immunohistochemistry demonstrated that this persisted for 4 weeks. GLO1 over-expression reduced MG-AGE levels at 6 h and 4 weeks, and GLO1 mice exhibited superior cardiac function at 4 weeks post-MI compared to WT mice. Immunohistochemistry revealed greater vascular density and reduced cardiomyocyte apoptosis in GLO1 vs. WT mice. The recruitment of c-kit$^+$ cells and their incorporation into the vasculature (c-kit$^+$CD31$^+$ cells) was higher in the infarcted myocardium of GLO1 mice. MG-AGEs appeared to accumulate in type I collagen surrounding arterioles, prompting investigation in vitro. In culture, the interaction of angiogenic bone marrow cells with MG-modified collagen resulted in reduced cell adhesion, increased susceptibility to apoptosis, fewer progenitor cells, and reduced angiogenic potential. This study reveals that MG-AGEs are produced post-MI and identifies a causative role for their accumulation in the cellular changes, adverse remodeling and functional loss of the heart after MI. MG may represent a novel target for preventing damage and improving function of the infarcted heart.

Keywords Advanced glycation end-products · Bone marrow cells · Extracellular matrix · Glyoxalase-1 · Methylglyoxal · Myocardial infarction

✉ Erik J. Suuronen
esuuronen@ottawaheart.ca

[1] Division of Cardiac Surgery, University of Ottawa Heart Institute, 40 Ruskin Street, Ottawa K1Y4W7, Canada

[2] Department of Cellular and Molecular Medicine, University of Ottawa, 501 Smyth Road, Ottawa K1H 8M5, Canada

[3] Biomedical Polymers Laboratory, and Jiangsu Key Laboratory of Advanced Functional Polymer Design and Application, College of Chemistry, Chemical Engineering and Materials Science, Soochow University, Ren-Ai Road 199, Suzhou Industrial Park, Suzhou 215012, China

[4] Diabetes Research Center and Departments of Internal Medicine and Pathology, Albert Einstein College of Medicine, 1300 Morris Park Avenue, Bronx, NY 10461, USA

[5] Geisel School of Medicine at Dartmouth, PreventAGE Healthcare, 16 Cavendish Court, Lebanon, NH 03766, USA

[6] Diabetes and Atherosclerosis Laboratory, University of Ottawa Heart Institute, 40 Ruskin Street, Ottawa K1Y4W7, Canada

Introduction

Ischemic cardiomyopathies, such as myocardial infarction (MI), are a leading cause of heart failure [21]. Despite timely pharmacologic or surgical intervention post-MI, the loss of viable myocardium from both the initial ischemic event and subsequent infarct expansion can lead to global remodeling and loss of function in many patients [20, 21]. Thus, discovering novel targets that provide cardioprotection or improve post-MI healing are highly desirable.

A growing body of evidence suggests a role for advanced glycation end-products (AGEs) in cardiovascular disease, though the majority of the work to date has

focused on diabetes and its associated cardiovascular complications [35]. In diabetes, methylglyoxal (MG) has been shown to have many intra- and extracellular targets with numerous deleterious effects including cell death, inflammation, and impaired angiogenesis [35]. Surprisingly little attention has been given to AGEs in the setting of non-diabetic ischemic cardiomyopathies such as MI [35]. AGEs have been linked with the severity and prognosis of heart failure, and AGE accumulation has been associated with 1-year incidence of major cardiac events and death following MI [19, 31]. However, a mechanistic or causative role for AGEs in cardiovascular disease, particularly in MI, is unclear.

AGEs are proteins that are non-enzymatically modified through glycation [34]. These modifications can alter protein structure and function leading to cellular and tissue dysfunction, a process also referred to as dicarbonyl stress [14, 35]. MG is likely the most important AGE precursor; and the major product of MG-specific glycation is hydroimidazolone (MG-H1), accounting for approximately 90% of all adducts [34]. MG is mostly produced as a degradation product of triose phosphates during glycolysis, and in normal physiologic conditions it is rendered inert primarily by the enzyme glyoxalase-1 (GLO1) [34]. However, hyperglycemia, hypoxia, ischemia, inflammation and oxidative stress stimulate the production of MG, while simultaneously inhibiting the activity of GLO1, leading to intra- and extra-cellular accumulation of MG and MG-derived AGEs (MG-AGEs) [35, 46]. Ischemia, inflammation and oxidative stress are all present post-MI, and the infarcted heart undergoes a metabolic shift to derive ATP from anaerobic glycolysis [22, 29], all of which are favourable for the formation of MG.

Based on this knowledge, we hypothesized that MG is produced post-MI and that it contributes to adverse ventricular remodeling and cardiac dysfunction. We aimed to determine if reducing MG-AGE accumulation through GLO1 over-expression could improve cardiac remodeling and mitigate functional loss in a mouse model of MI. We demonstrate that MG-AGEs accumulate in the heart post-MI; and limiting this process by over-expressing GLO1 in the vasculature and bone marrow leads to preserved ventricular geometry and cardiac function. Furthermore, we report that MG-AGE modification of collagen in the extracellular matrix (ECM) of the myocardium, and impairment of progenitor cell recruitment and neovascularization contribute to the harmful effects of MG post-MI. Thus, this study establishes a role for MG in the cellular changes, adverse remodeling and functional loss of the infarcted heart.

Materials and methods

Transgenic hGlo1 mice

This study uses human GLO1 over-expressing mice (GLO1 mice) bred on a C57/BLJ6 background, which carry a transgene encoding *hGlo1* with a cMyc epitope tag under the control of the preproendothelin-1 promoter, as previously described [42]. This promoter is appropriate because it is highly expressed in the vasculature and it is up-regulated in the infarcted heart [17, 39]. This mouse model and its characterization have been previously reported by our lab and others [13, 15, 42, 43]. Briefly, hGLO1 expression was detected in all tissues tested: the heart, aorta, kidney, eye, liver and brain [42]. Despite the reported endothelial-specific expression of the preproendothelin-1 promoter, GLO1 activity was fivefold greater in endothelial cells, smooth muscle cells and cells of bone marrow origin in these mice [42, 43]. Within the heart, GLO1 overexpression was not detected in cardiomyocytes, but was confirmed in the vasculature [43]. In whole heart, GLO1 mice showed a 1.8-fold increase in GLO1 activity ($p = 0.002$; as measured by the rate of formation of *S*-D-lactoylglutathione from hemi-thioacetal), and no difference in the level of the GLO1 co-factor reduced glutathione ($p = 0.7$), compared to non-transgenic wild-type (WT) littermates [43]. Otherwise, no phenotypic differences were observed between GLO1 and WT mice. All experiments used female mice hemizygous for the *hGlo1* transgene or their non-transgenic wild-type (WT) littermates.

Myocardial infarction model

All the procedures were performed with the approval of the University of Ottawa Animal Care Committee and in accordance with the National Institutes of Health Guide for the Care and Use of Laboratory Animals. MI was induced in 9-week-old mice by a surgeon blinded to mouse genotype. Briefly, mice were anaesthetized under 2.5% isoflurane, intubated and kept under mechanical ventilation. A left-sided open thoracotomy was performed and the left anterior descending coronary artery was permanently ligated with a 7-0 silk suture 2 mm below the tip of the left auricle. MI was confirmed by myocardial blanching. Short acting buprenorphine (0.05 mg/kg) was administered subcutaneously at least an hour prior to surgery, and slow release buprenorphine (1.2 mg/kg) was administered subcutaneously immediately before surgery for peri-operative analgesia.

Echocardiography

Mice were anaesthetized under 2.5% isoflurane, intubated and kept under mechanical ventilation. Cardiac function was assessed by echocardiography on long-axis views with a Vevo770 system (VisualSonics, Toronto, Canada) in B mode with the use of a 707B series real-time microvisualization (RMV) scanhead probe.

MG-derived AGE determination

GLO1 and WT mice underwent surgical MI and the infarct zone tissue (blanched region) was harvested 6 h later from the myocardium. Tissue from age-matched non-infarcted controls was also procured. Tissue was surgical microdissected and immediately snap frozen in liquid nitrogen and kept at −80 °C until required. Samples were prepared for analysis by liquid chromatography-mass spectrometry by sequential proteolytic digestion as previously described [1]. Briefly, tissue was first mechanically homogenized using liquid nitrogen. Once crushed, an approximately equal volume of QQ water was added to the samples, which were then freeze-thawed three times (frozen at −80 °C, and thawed on ice) and then sonicated. Samples were kept at −80 °C until further processing. Prior to proteolytic digestion, sample protein concentrations were first assayed using the bicinchoninic acid method. For sample proteolytic digestion, samples were digested over a period of 5 days. On day 1500 µg of protein in 25, 10 µL of internal standard (provided by PreventAGE Health Care, LLC), 5 µL 2 mg/mL pepsin (Sigma), and 25 µL of 20 mM HCl were added to a 1 mL digestion vial then mixed. Samples were purged with N_2, vortexed and incubated at 37 °C for 24 h. On day 2, 8 µL of 65 mM KOH, 25 µL of 50 mM KPO_4 with gentamicin, and 5 µL of 2 mg/mL Pronase (Sigma) were added to the vials and mixed. Samples were purged with N_2 and incubated for 24 h at 37 °C. On day 3, 5 µL of 2 mg/mL Aminopeptidase (Sigma), 5 µL of 2 mg/mL Prolidase (Sigma) were added to the vials and mixed. Samples were purged with N_2 and incubated at 37 °C for 48 h. Following incubation, samples were transferred to cryovials for mass spectrometry. Mass spectrometry was carried out at PreventAGE Health Care, LLC (Dartmouth Regional Technology Center, Lebanon, NH 03766 USA) as described [4].

Histology and immunohistochemistry

Mice were sacrificed at 4 weeks. Hearts were collected, perfused with 2–3 mL of saline, snap frozen in O.C.T compound and stored at −80 °C. Slides were prepared with 8 µm sections at different levels. Masson Trichrome staining was performed to measure relative infarct size by the midline method, as previously described [36]. Unless otherwise specified, all primary antibodies for immunohistochemistry were purchased from Abcam and all Alexa fluor® (488, 546) secondary antibodies from Invitrogen. All tissue sections were fixed in cold acetone and washed with Tris-buffered saline with Tween® 20. Tissue sections were stained with antibodies against CD31 (1:50, for endothelial cells), α-smooth muscle actin (α-SMA; 1:200, for vascular smooth muscle cells), cardiac troponin I (1:200) + wheat-germ agglutinin (1:40, for cardiomyocytes) or c-kit (1:200, for progenitor cells). Apoptotic cells were identified using an anti-active caspase 3 antibody (1:300) or TUNEL staining (Roche; following manufacturer's protocol). Cell nuclei were stained with DAPI. Images were acquired with a Zeiss Z1 fluorescence microscope and analyzed by AxioVision digital image software. For quantification, six random microscopic fields-of-view were counted per sample in a blinded fashion. An anti-methylglyoxal-derived AGE antibody (MG-AGE 3D11; Cellbiolabs STA-011) and an anti-type I collagen antibody were used to identify MG-AGE modified collagen, as described [37]. Briefly, frozen tissue sections were fixed in acetone and washed with Tris-buffered saline with Tween® 20. To reduce background, goat anti-mouse IgG (1:25 dilution) in 10% fetal bovine serum in phosphate buffered saline was used to block sections for 3 h prior to incubating with the primary antibody overnight at 4 °C.

A subset of mice was sacrificed 24 h after ligation surgery for the determination of acute infarct size by triphenyl tetrazolium chloride (TTC) staining. Hearts were excised, washed with phosphate buffered saline, frozen at −20 °C, and then cut into 1 mm thick slices. Slices were incubated with 1% 2,3,5-triphenyl tetrazolium chloride and fixed in 10% formalin. Images were taken and infarct size was measured using Image J software.

Collagen gels and methylglyoxal glycation

Collagen type I (1%; Nippon Ham) gels were prepared as previously described [3]. Briefly, 1% porcine collagen I gels were prepared in phosphate buffered saline and the pH was adjusted to 7.2–7.4. A thin layer of gel was coated at the base of a well in six-well dishes and incubated at 37 °C in a humidified chamber for 2 h. Subsequently, gels were incubated overnight at 37 °C with phosphate buffered saline or with 1 mM MG (Sigma). This concentration is effective at generating glycated collagen in vitro to an extent that is comparable to in vivo levels of glycated collagen in the ventricles of rats with diabetic cardiomyopathy [37], thus demonstrating that 1 mM MG is physiologically relevant. Glycation of the gel was confirmed by Western blot (data not shown) using a monoclonal antibody (1H7C6) against MG-H1 adducts (the major MG

adducts), kindly provided by Drs. Xue-Liang Du and Michael Brownlee (Albert Einstein College of Medicine, Bronx, USA).

Peripheral blood mononuclear cells and in vitro studies

Procedures for isolating human peripheral blood mononuclear cells (PBMCs) were approved by the Human Research Ethics Board of the University of Ottawa Heart Institute. With informed consent, total PBMCs were isolated from the blood of healthy volunteers, and cultured for 4 days on fibronectin, as previously described [25]. PBMCs were then cultured on MG-modified or non-modified collagen gels in endothelial growth medium-2 (EGM-2) with fetal bovine serum, vascular endothelial growth factor, R^3-insulin growth factor and endothelial growth factor supplements (Lonza) at 37 °C, after which cells and/or conditioned media were collected. PBMCs were evaluated for viability and phenotype (by flow cytometry), adhesion, and angiogenesis, as described below.

CAC viability, chemotaxis and adhesion

For viability, PBMCs were cultured on collagen gels (±MG modification) for 2 days under serum deprivation and hypoxic conditions as described [25]. Cells were then stained for CD133, CD34, CD31, CD144 and 7-aminoactinomycin (7-AAD) and analyzed by flow cytometry. For adhesion, 5×10^5 DAPI-stained PBMCs were seeded on MG-modified or non-modified collagen gels for 60 min, fixed with 4% paraformaldehyde and counted per field-of-view in a blinded fashion (20× magnification). For chemotaxis, PBMCs on the two collagen gels were serum starved overnight, then lifted and placed in the upper chamber of Transwell® Permeable Supports (Corning), with 0.05 μg/mL of vascular endothelial growth factor (Cedarlane) in EBM in the bottom chamber as the migratory stimulus, as previously described [25]. After overnight culture, PBMCs were fixed with paraformaldehyde and the number of migrating cells was quantified.

Flow cytometry

Flow cytometry was performed with a FACSAria™ (BD Biosciences) as described previously [25]. Briefly, for human PBMCs, phenotype was assessed at baseline and after 4 days culture on collagen gel (±MG modification). Cells were lifted and stained for CD31, CD34, CD133 and CD144 for 30 min at 4 °C in Hank's balanced saline solution, then washed and re-suspended in 0.5% bovine serum albumin in Dulbecco's phosphate buffered saline for immediate analysis by flow cytometry. Antibodies used were: CD31-FITC (Beckman Coulter), CD34-PE-Cy7 (eBioscience), CD133-APC (Miltenyi Biotec), CD144-PE (Beckman Coulter) with matched Isotype controls. Data were analyzed using FACSDiva software. For mice, circulating PBMCs were collected from mice by saphenous vein bleeds pre-operatively and at days 2, 7, and 28 post-surgery, as described previously [42]. The mononuclear cell fraction was labeled with antibodies against the following antigens: c-kit (Southern Biotech, Birmingham, USA), CD45 (BD Biosciences, Mississauga, Canada), and flk-1 (mouse vascular endothelial growth factor receptor-2; eBioscience, San Diego, USA), and analyzed by FACSAria™.

In vitro angiogenesis assay

PBMCs were stained with DAPI and human umbilical vein endothelial cells (Invitrogen) were labeled with CellTracker Orange™ (Invitrogen) prior to the in vitro ECMatrix™ assay (Millipore). Human umbilical vein endothelial cells (5×10^3 cells) were seeded with PBMCs (5×10^3 cells; from collagen gel ± MG modification) in μ-slide angiogenesis slides (Ibidi) coated with 10 μL of ECMatrix™, prepared following the manufacturer's protocol. The number of $DAPI^+$ PBMCs contributing to structure formation (co-localization of DAPI and CellTracker™ Orange) and total tubule length were quantified per field-of-view (10× magnification) after overnight culture. Each condition was assayed in triplicate, with a minimum of $n = 4$ per condition.

Statistical analysis

Statistical analyses were performed using GraphPad Prism 6 software. All results are expressed as the mean ± standard error, and the sample size (n) for each experiment is provided in the figure legends. Unless otherwise indicated, for single comparison of data between 2 groups a two-tailed student's t test was performed. For multiple comparisons, a one- or two-way analysis of variance with a Bonferroni or Tukey correction was applied. Due to inherent variability in donors and flow cytometry, data for PBMC mobilization in mouse peripheral circulation was analyzed using a t test at each time-point, and for human PBMCs, data was reported as the mean fold-change of treatment-to-control ± standard error, and analyzed using ratio paired t tests. The identification of outliers in the data was planned a priori and was performed by the identify outlier function in the Graphpad Prism 6 software using the ROUT method with a maximum false discovery rate of 5%. This resulted in the exclusion of one data point in the mouse PBMC flow cytometry analysis. Probability values of $p < 0.05$ were considered statistically significant.

Results

MI stimulates MG-H1 production, and GLO1 over-expression preserves cardiac function

Myocardial tissue was harvested from GLO1 over-expressing mice and their WT littermates at baseline (no MI) and 6 h post-MI and mass spectrometry was performed to measure AGE content (MG-H1, the MG-derived carboxyethyl-lysine and the glyoxal-derived carboxymethyl-lysine). At 6 h post-MI, there was a 52% increase in myocardial MG-H1 content in WT mice compared to non-infarct controls, whereas MG-H1 levels were unchanged in GLO1 mice post-MI compared to GLO1 and WT mice at baseline (Fig. 1a). For carboxymethyl-lysine and carboxyethyl-lysine, myocardial levels did not change in WT mice after MI; but in post-MI GLO1 mice their abundance was reduced (Fig. 1b, c). To visualize the extent of MG-H1 accumulation over time, immunohistochemistry was performed on myocardial tissue sections of GLO1 and WT mice at 4 weeks post-MI. Diffuse MG-H1 staining was qualitatively observed within the granulation tissue and in arterioles and cardiomyocytes of the infarct scar; however, less MG-H1 staining intensity was observed in GLO1 compared to WT mice (Fig. 1d). Therefore, MI acutely stimulates the production of MG-AGEs and their presence appears to persist in the myocardium for up to 4 weeks.

Although GLO1 over-expression reduced MG-H1 production at 6 h post-MI in the GLO1 mice, there was no difference in the acute infarct size between GLO1 and WT mice at 24 h post-MI as determined by TTC staining (Fig. 2a, b), indicating that GLO1 and WT mice sustained the same initial injury. However, reducing MG-AGE levels in the myocardium post-MI (via GLO1 over-expression) significantly limited cardiac dysfunction over the 4-week observation period. Notably, echocardiography revealed greater left ventricular ejection fraction in GLO1 mice compared to WT mice at both 1 and 4 weeks post-MI (Fig. 2c). A higher % fractional area change and a reduction in end-systolic volumes were also observed in GLO1 mice at 4 weeks post-MI (Fig. 2d, e). There were no differences in end-diastolic volume, cardiac output, left ventricular mass and heart rate between GLO1 and WT mice (Fig. 2f–i). Together, these results demonstrate that MG-AGEs are produced and accumulate in the post-MI myocardium, and that GLO1 over-expression can prevent their accumulation and limit the loss of cardiac function.

GLO1 over-expression reduces scar size and cell death

Masson Trichrome staining revealed that GLO1 mice had a reduced final scar size compared to WT mice at 4 weeks post-MI (Fig. 3a, b). GLO1 over-expression also reduced on-going cell death in the myocardium (Fig. 3c–g). At 4 weeks, less apoptotic active caspase-3$^+$ cardiomyocytes were present in the infarct zone of GLO1 mice compared to WT littermates (Fig. 3c), and TUNEL staining confirmed the reduced cardiomyocyte cell death in GLO1 mice (Fig. 3d). The number of TUNEL$^+$ non-cardiomyocyte cells was also reduced in GLO1 vs. WT mice (Fig. 3e). Overall, GLO1 over-expression decreased final scar size and reduced on-going cell death in the myocardium.

Vascular density and c-kit$^+$ cell number is enhanced in GLO1 mice post-MI

In diabetes, MG has been shown to impair angiogenesis [9]; therefore, vascular density was assessed in the hearts of GLO1 and WT mice to determine if MG played a similar role post-MI. In non-infarcted hearts, no difference was observed in vascular density between GLO1 and WT mice (data not shown). However, at 4 weeks post-MI, GLO1 mice had a greater number of CD31$^+$ capillaries and α-SMA$^+$ arterioles in the infarct area compared to WT (Fig. 4a–c). To understand the mechanism, the bone marrow repair response was examined, since others have shown that bone marrow c-kit$^+$ cells play a major role in vascular repair post-MI [10, 11]. Therefore, PBMCs were collected from mice at 0, 2, 7 and 28 days post-MI to assess the mobilization of c-kit$^+$, c-kit$^+$VEGFR2$^+$CD45$^-$ and c-kit$^+$VEGFR2$^+$CD45$^+$ cells over time. There were non-statistically significant increases in the number of circulating c-kit$^+$ and c-kit$^+$VEGFR2$^+$CD45$^-$ cells at 7 days post-MI in GLO1 mice ($p = 0.055$ and 0.056, respectively), while the number of c-kit$^+$VEGFR2$^+$CD45$^+$ cells was significantly greater in GLO1 mice vs. WT at 7 days (Fig. 4d–f). To determine the contribution of c-kit$^+$ cells to neovascularization in the infarct area of the MI heart, immunohistochemistry was performed (Fig. 4g–k). GLO1 mice had more arterioles with c-kit$^+$ cells incorporated around the vessel vs. WT mice (Fig. 4g), and the number of c-kit$^+$ cells that were localized within these arterioles was increased in GLO1 mice (Fig. 4h). The number of c-kit$^+$ cells that co-stained with endothelial marker CD31$^+$ was greater for GLO1 mice vs. WT (Fig. 4i), as was the overall number of c-kit$^+$ cells recruited to the myocardium (Fig. 4j). Together, these results suggest that GLO1 over-expression promotes post-MI neovascularization possibly through increased recruitment and/or survival of c-kit$^+$ cells.

MG modification of ECM proteins impairs the angiogenic properties of PBMCs

Extensive ECM remodeling post-MI leads to scar deposition, consisting mainly of type I collagen, and collagen is a major target for MG-mediated glycation [12, 37]. By

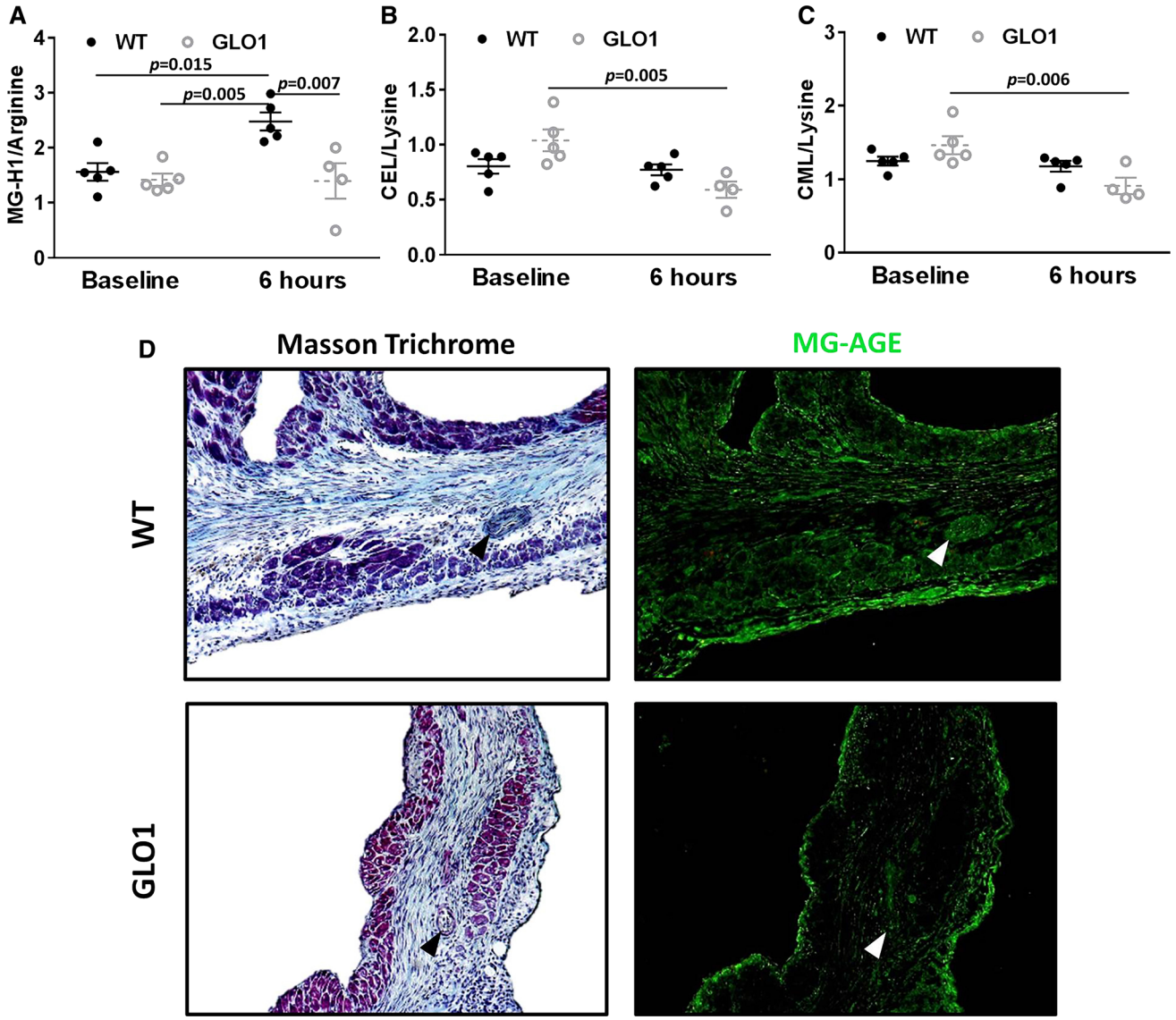

Fig. 1 MG and AGEs accumulate in the myocardium post-MI. Levels of the following AGEs: MG-H1 (**a**), carboxyethyl-lysine (CEL) (**b**) and carboxymethyl-lysine (CML) (**c**) in the infarct tissue of mice at 6 h post-MI measured by mass spectrometry ($n = 4$–5). **d** Masson-Trichrome and MG-AGE stained serial tissue sections in the infarct zone at 4 weeks post-MI. *Arrowheads* indicate arterioles. Data are presented as mean ± standard error

fluorescence immunohistochemistry, prominent MG-H1 accumulation was observed surrounding arterioles in the border zone of the infarcted myocardium at 4 weeks post-MI (Fig. 5a). More co-localization of MG-H1 and collagen I staining, particularly surrounding the arterioles, was qualitatively observed in WT compared to GLO1 mice (Fig. 5a). Collagen glycation has been shown to impair neovascularization by endothelial cells in collagen gels in vitro and in vivo [12]. Therefore, some in vitro experiments were performed to investigate how MG-modified collagen may affect the phenotype and function of PBMCs recruited to the heart post-MI. For clinical relevance, human PBMCs were cultured on MG-modified or non-modified type I collagen. Exposure to MG-modified collagen had no effect on their chemotactic response towards vascular endothelial growth factor (data not shown); however, fewer PBMCs were capable of adhering to MG-modified collagen vs. non-modified collagen (Fig. 5b). To evaluate if MG-modified collagen impaired angiogenic potential, PBMCs from either substrate were added together with human umbilical vein endothelial cells in an angiogenesis assay. With PBMCs from the MG-modified collagen there was reduced total capillary-like network length and less of these PBMCs incorporated into capillary-like structures compared to PBMCs from non-modified collagen (Fig. 5c–e). Therefore, the interaction of

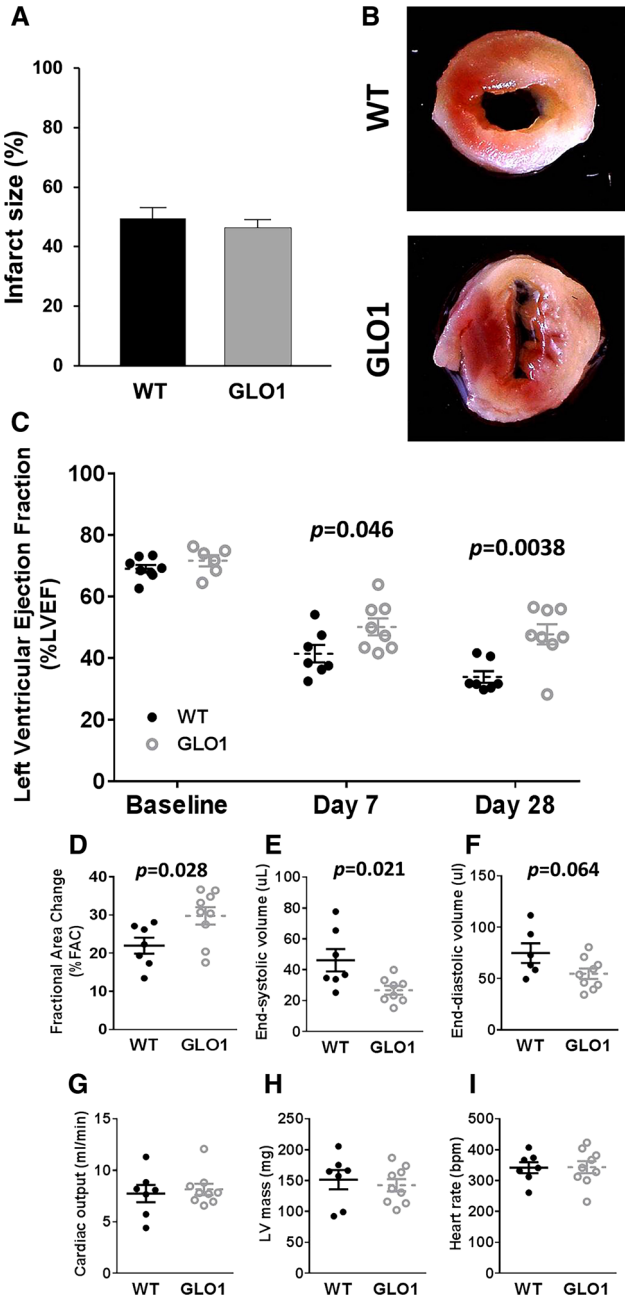

Fig. 2 Preventing MG-AGE accumulation through GLO1 overexpression preserves cardiac geometry and function. **a** Infarct size in GLO1 and WT mice at 1 day post-MI ($n = 5$). **b** Representative images of TTC-stained heart sections at 1 day post-MI. Echocardiography assessment of left ventricular ejection fraction (LVEF) (**c**), fractional area change (**d**), end-systolic volume (**e**), end-diastolic volume (**f**), cardiac output (**g**), left ventricular mass (**h**), and heart rate (**i**) in WT and GLO1 mice at 4 weeks post-MI (GLO1 $n = 8$, WT $n = 7$). Data are presented as mean ± standard error

PBMCs with MG-modified collagen reduces their angiogenic potential, which appears consistent with the in vivo observations.

PBMCs were subjected to apoptosis-inducing conditions similar to myocardial ischemia (serum/growth factor deprivation and hypoxia). Culture in these conditions for 2 days did not affect the overall viability of PBMCs, although the endothelial cell fraction ($CD31^+$, $CD144^+$ and $CD31^+CD144^+$ cells) from MG-modified collagen exhibited reduced survival compared to non-modified collagen culture (Fig. 6a–c). The effect of MG-modified collagen on the putative $CD133^+$ and $CD34^+$ progenitor cell subpopulations that participate in post-natal vasculogenesis [10] was also examined. There was reduced viability of $CD34^+$ cells and $CD133^+$ cells in PBMCs cultured on MG-modified collagen under apoptotic conditions (Fig. 6d, e). When cultured for 4 days under normal conditions, PBMCs on MG-modified collagen had a reduced proportion of $CD34^+$ and $CD133^+$ cells compared to non-modified collagen culture suggesting loss of this phenotype (Fig. 6f, g). Together these experiments highlight potential negative effects that glycated collagen may have on the angiogenic potency of PBMCs.

Discussion

This study sought to determine if MG production post-MI has a role in adverse remodeling and cardiac dysfunction. The main findings are that: (1) MG-AGEs are produced soon after MI and accumulate in the myocardium; (2) overexpressing GLO1 prevents MG-AGE production and accumulation post-MI resulting in less cell death, reduced scar size and preserved cardiac function; (3) GLO1 overexpression promotes greater c-kit^+ cell recruitment and higher vascular density; and (4) MG-modified collagen impairs the angiogenic properties of PBMCs. Taken together, this provides evidence that MG-AGEs are produced acutely post-MI and their accumulation contributes to ongoing cardiac remodeling and dysfunction.

The toxic effects of MG have been researched widely in aging, and most extensively in diabetes [28, 35]. Knowledge of the role that dicarbonyl stress plays in diabetic cardiovascular disease is expanding, but comparatively little is known of it in non-diabetic heart disease [18, 19, 35]. In one clinical study, carboxymethyl-lysine levels in the plasma of patients with congestive heart failure were correlated with the severity and prognosis of the disease [19]. In other work, higher MG-H1 levels were detected in human carotid atherosclerotic plaques associated with a rupture-prone phenotype [16]. Of the few animal studies reported, use of a transient cardiac ischemia mouse model showed that ischemia led to increased MG and AGE production in the myocardium, but it did not establish whether MG or its AGEs participated in cardiac remodeling [2]. As such, it remains undetermined whether MG and its AGEs constitute a biomarker or contribute to cardiac remodeling and loss of function post-MI.

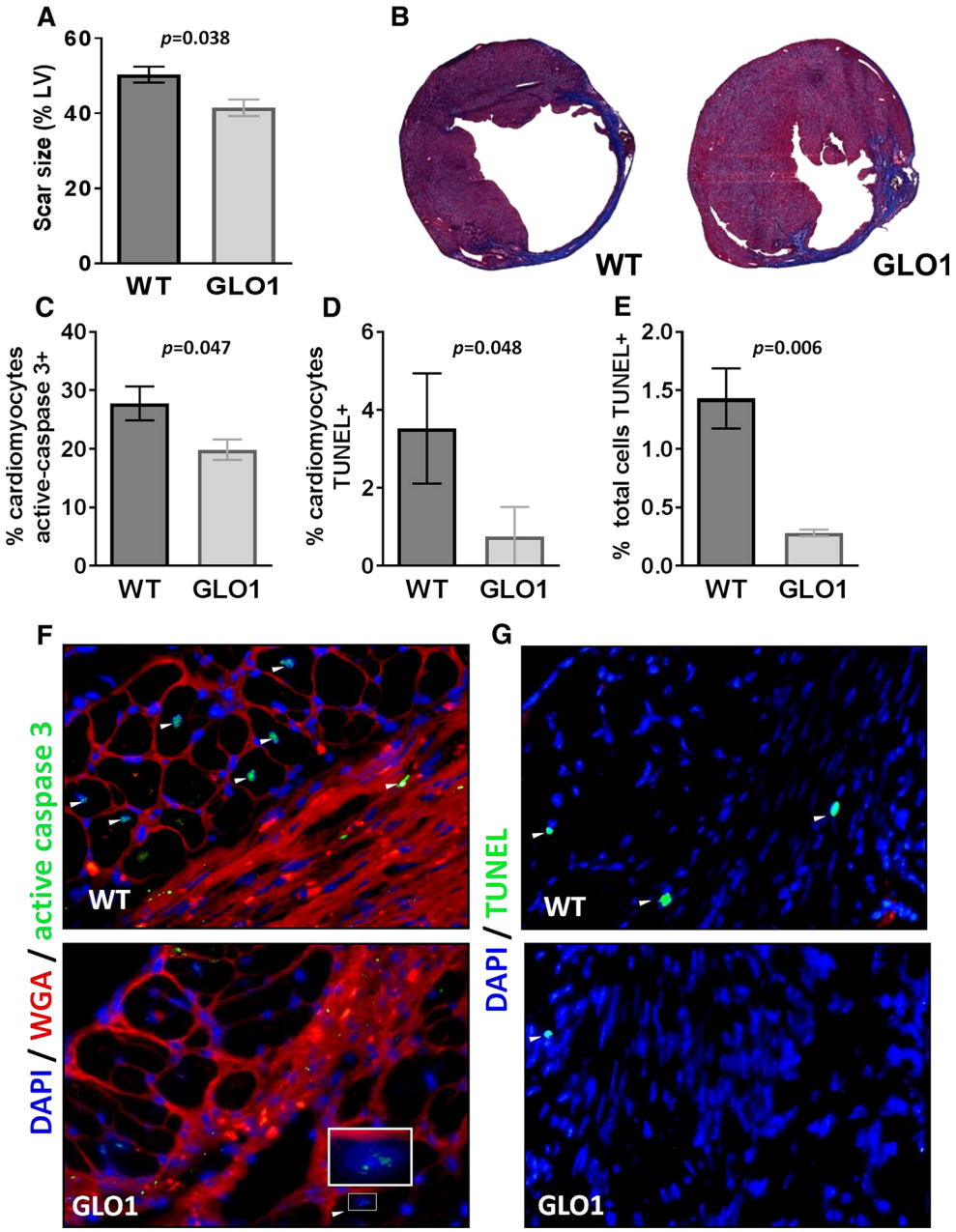

Fig. 3 GLO1 over-expression reduces infarct scar size and cell death in mice post-MI. **a** Scar size in GLO1 and WT mice at 4 weeks post-MI ($n = 5$). **b** Representative Masson-Trichrome stained tissue sections at 4 weeks post-MI. Proportion of apoptotic active caspase 3^+ cardiomyocytes (**c**), $TUNEL^+$ cardiomyocytes (**d**), and $TUNEL^+$ non-cardiomyocyte cells (**e**) in tissue sections at 4 weeks post-MI in the infarct zone, determined by immunohistochemistry ($n = 5$). **f** Representative images of apoptotic cardiomyocytes (active caspase 3^+, *green*, *arrowheads*) in WT and GLO1 mice. The *highlighted area* (*white box*) has been magnified to show representative co-localization of DAPI (*blue*) and active caspase-3 staining. **g** TUNEL staining (*green*, *arrowheads*) of non-cardiomyocyte cells. Data are presented as mean ± standard error

Our results present the argument that, though AGEs may initially be a consequence of MI, MG-AGEs are also a contributor to the ensuing cellular changes, LV remodeling and deterioration of cardiac function. We observed functional benefits of GLO1 over-expression as early as 1 week, which persisted to 4 weeks post-MI. This suggests that MG-AGE accumulation was deleterious from the onset of ischemia. The progressive loss of contractility and increased dilatation with maintained cardiac output seen in the WT cohort may be indicative of early stage heart failure [24]. In contrast, the protective effect of GLO1 over-expression may either delay this process or altogether prevent it; however, a comparison of the progression to heart failure remains to be investigated in future long-term studies. Overall our results link MG-AGE accumulation to the negative remodeling and progressive loss of cardiac function post-MI.

Identifying a precise mechanism for the action of MG is challenging, as MG affects numerous signaling pathways and cell functions [35]. Furthermore, many of the reported in vitro studies have used MG concentrations that far exceed (patho)physiological levels [33], possibly confounding the interpretation of the in vivo actions of MG. Our GLO1 transgenic mouse model provides the advantage of studying physiologically relevant concentrations of MG and its consequences in the pathology of disease. For example, we

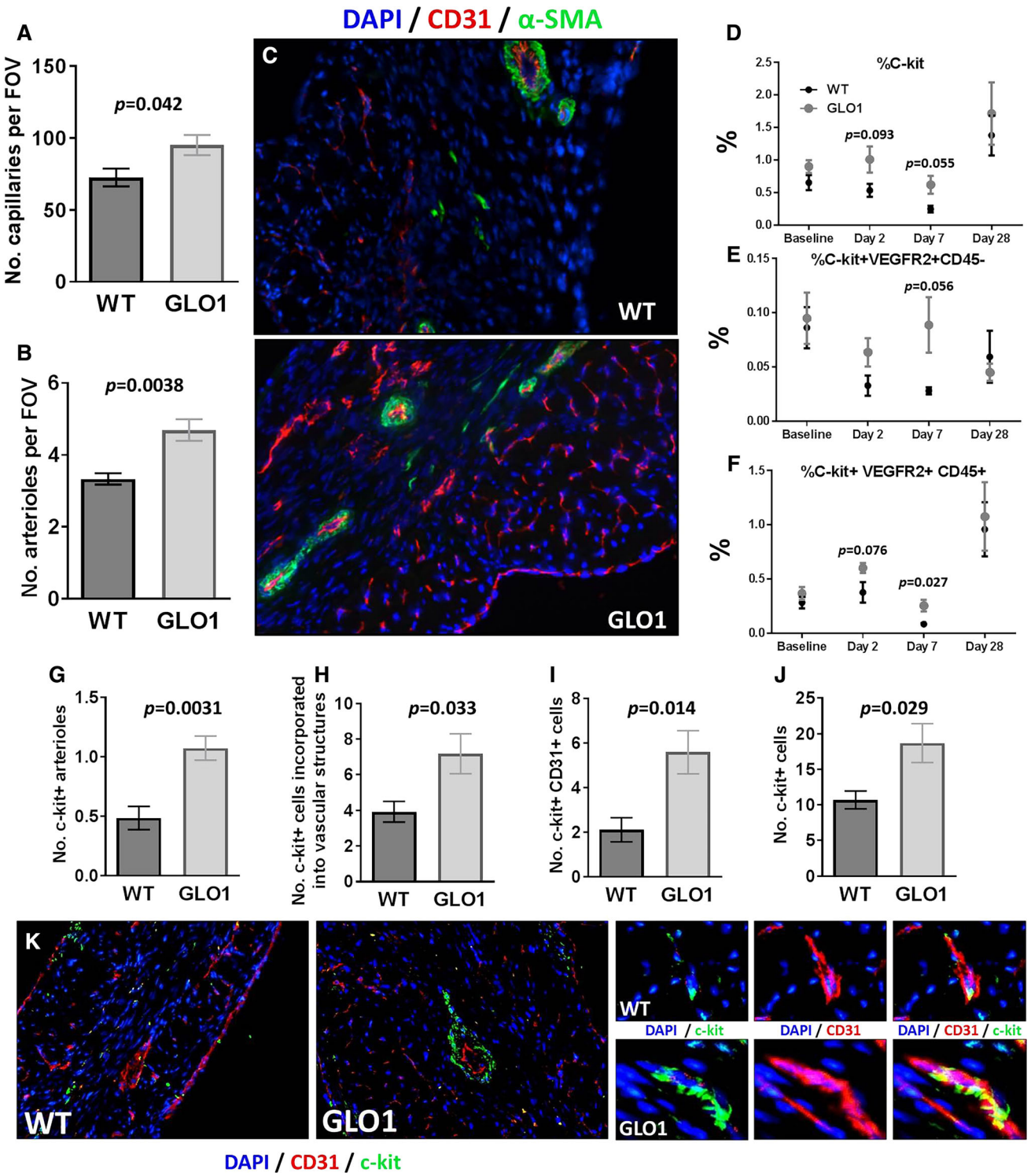

Fig. 4 GLO1 over-expression increases vascular density, and recruitment and vascular contribution of c-kit$^+$ cells in the MI heart. **a**, **b** Number of capillaries (CD31$^+$) and arterioles (α-SMA$^+$CD31$^+$) in the infarct zone by immunohistochemistry ($n = 5$). **c** Fluorescence microscopy images of α-SMA$^+$ arterioles (*green*) and CD31$^+$ capillaries (*red*). **d–f** Percentage of PBMCs in the peripheral circulation that are c-kit$^+$, c-kit$^+$VEGFR2$^+$CD45$^-$ and c-kit^{+-} VEGFR2$^+$CD45$^+$ over a period of 4 weeks post-MI assessed by flow cytometry ($n = 3$–5). The number of arterioles containing c-kit$^+$ cells (**g**), c-kit$^+$ cells incorporated into arterioles (**h**), c-kit$^+$CD31$^+$ cells (**i**), and total number of c-kit$^+$ in the infarcted myocardium (**j**) at 4 weeks post-MI ($n = 5$). **k** *Left panels* infarct zone images of recruited c-kit$^+$ cells (*green*) co-stained with CD31 (*red*). *Right panels* higher magnification images. Data are presented as mean ± standard error

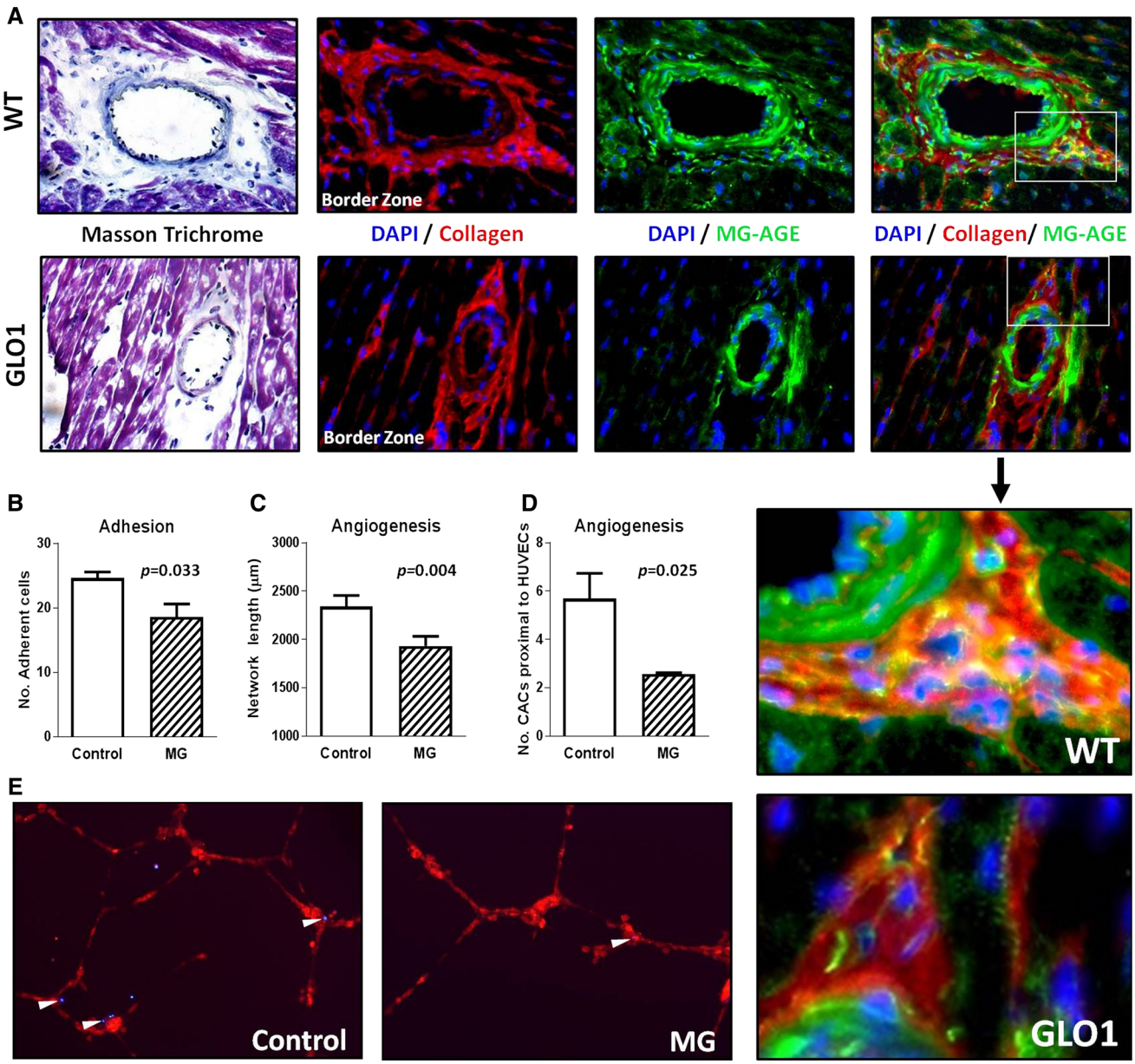

Fig. 5 MG glycates collagen in vivo and impairs pro-angiogenic properties of cultured human PBMCs in vitro. **a** Masson-Trichrome and immunofluorescence images [MG-AGE (*green*) and collagen type I (*red*)] of the MI border zone. *Highlighted areas* of the last panels (*white boxes*) have been magnified in the images below, showing greater co-localization of collagen and MG-AGE (*yellow*/*orange*) surrounding an arteriole in a WT mouse. **b** Number of human PBMCs adhered to control (non-modified collagen) and MG-modified collagen after 1 h in vitro ($n = 4$). **c** Number of PBMCs proximal to HUVEC structures, **d** total network length, and **e** representative images of an angiogenesis assay using HUVECs co-cultured with PBMCs from control or MG-modified collagen culture (PBMCs stained *blue* and HUVECs *orange*; $n = 5$). Data are presented as mean ± standard error

recently reported that MG contributes to the development of diabetic cardiomyopathy through inflammation and endothelial cell death in a mouse model of type 1 diabetes [43]. In the literature, MG has been shown to influence cell death and apoptosis, to impair angiogenesis and neovascularization, and to modify and impair ECM signaling [34, 35]. Since these are prominent processes in post-MI cardiac remodeling, we investigated them in the present study.

Apoptosis during cardiac remodeling (independent of the immediate post-MI necrotic death) contributes to myocardial ischemia and heart failure [23, 45]. In heart failure, usually less than 1% of cells are dying at a given time, leading to a progressive loss of cardiomyocytes and deterioration of the heart [23]. Expression of the apoptotic effector active caspase-3 is increased in heart failure patient hearts, and its over-expression in a mouse MI model

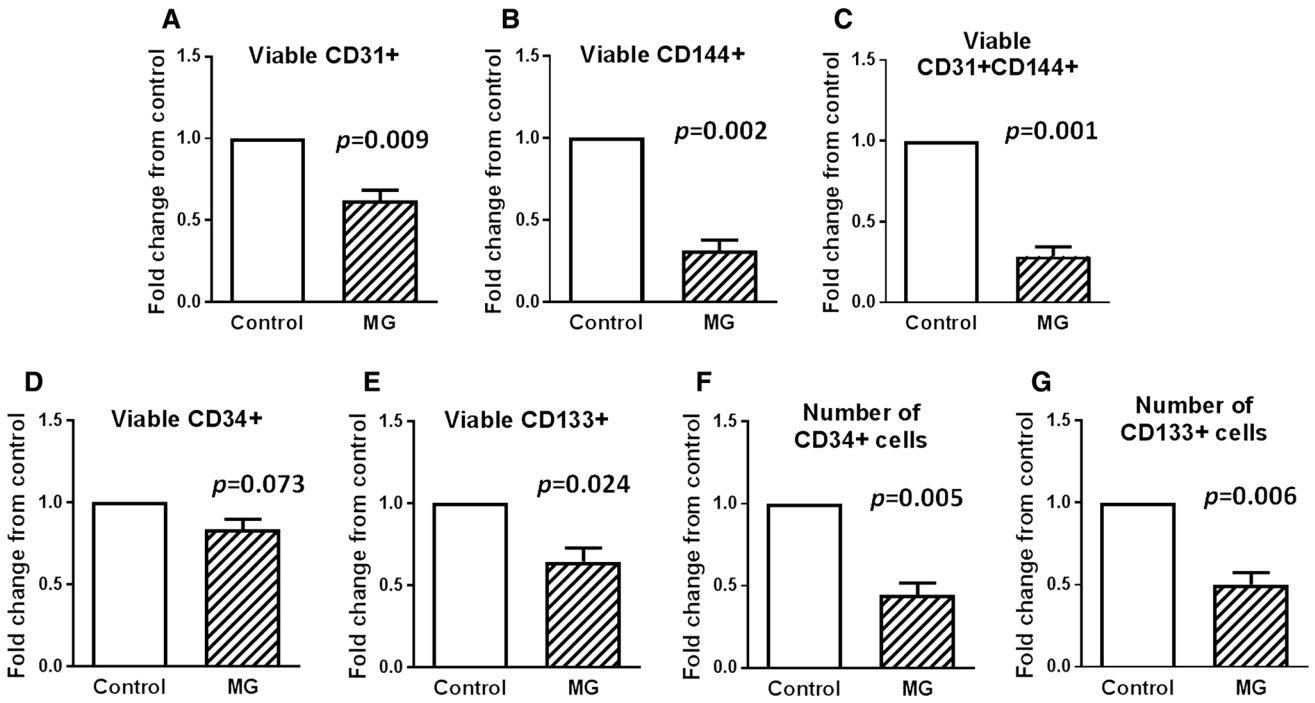

Fig. 6 MG-modified collagen impairs cell survival and phenotype in vitro. **a–e** Viability of the $CD31^+$, $CD144^+$, $CD31^+CD144^+$, $CD34^+$ and $CD133^+$ fractions of PBMCs cultured on control or MG-modified collagen and subjected to apoptotic conditions ($n = 5$). **f**, **g** Number of $CD34^+$ and $CD133^+$ cells after PBMCs were cultured on control or MG-modified collagen for 4 days ($n = 5$). Data are presented as mean ± standard error

increased scar size and reduced cardiac function [7]. Moreover, MG-AGEs have been shown to induce caspase-3 activation and cardiomyocyte apoptosis via oxidative stress [27]. In our study, the death of cardiomyocytes and non-cardiomyocyte cells was reduced (less active caspase-3^+ and $TUNEL^+$ cells) in GLO1 mice post-MI demonstrating the potential for GLO1 over-expression to confer protection from apoptosis. Limiting the on-going cell death in the myocardium may partially explain the functional benefits and reduced infarct size in GLO1 mice. Whether these effects are the result of a direct action of GLO1 or secondary to other mechanisms is unclear. A likely scenario is that multiple GLO1-mediated factors contribute to preserving myocardial viability, including secondary effects of improved post-MI neovascularization.

Numerous studies report that MG impairs angiogenesis in diseases such as diabetes [30, 35, 42–44]. Our results suggest that similar MG-mediated anti-angiogenic mechanisms exist in MI, and that limiting the production of MG-AGEs (via GLO1 over-expression) can increase vascularity. The presence of c-kit^+ cells, their adoption of an endothelial phenotype (c-kit^+CD31^+) and their incorporation into arterioles in the infarcted heart was greater in GLO1 mice compared to WT mice. Although we did not identify the source of these cells, the recruitment of mobilized bone marrow c-kit^+ cells has been shown to increase capillary density, reduce remodeling and improve function in MI mice [11, 32]. Increased numbers of circulating c-kit^+ cells were observed at 7 days post-MI in GLO1 mice, therefore, greater mobilization and recruitment of these cells to the infarcted myocardium is a possibility. Furthermore, it is likely that bone marrow cells of GLO1 mice recruited to the infarcted myocardium are protected in the high dicarbonyl stress environment and have improved pro-angiogenic capacity, as we have previously demonstrated with these transgenic mice [42]. Nevertheless, our results cannot exclude a contribution from c-kit^+ cardiac stem cells originating from the myocardium, which have also been shown to possess greater pro-angiogenic function in GLO1 mice [30].

MG modification of the cardiac ECM may also be an important contributor to cardiovascular disease given that it has a >10-fold longer turn-over than other cardiac proteins [37, 47]. Arginine residues within the integrin recognition domains of collagen constitute major targets for MG-mediated glycation [40, 41], potentially disrupting cell-ECM interactions that are essential for cell phenotype and function [8]. Notably, collagen glycation has been shown to negatively affect angiogenesis and vascular repair in vitro and in vivo [12, 26], but this has not been established in the context of MI. In our study, GLO1 mice had decreased MG-AGE content in the infarct area (which consists primarily of collagen type I), and a reduction in MG-AGE modified collagen surrounding the vasculature in

the border zone, compared to WT mice. This suggests that MG-modification of collagen in the cardiac ECM may contribute to defective neovascularization post-MI, which was supported by our in vitro studies using human PBMCs. MG-modified collagen supported less PBMC adhesion and impaired their angiogenic potential. Furthermore, collagen glycation has been shown to induce endothelial cell anoikis (cell death resulting from detachment) [9], and we similarly observed reduced viability of $CD133^+$ progenitors and $CD31^+$ and $CD144^+$ endothelial fractions in PBMCs cultured on MG-modified collagen under apoptosis-inducing conditions. Taken together, our results suggest that MG-mediated collagen glycation may interfere with cell-ECM interactions and limit the recruitment, viability and function of angiogenic cells leading to reduced vascularization in the MI heart.

A limitation of our study is that elevated GLO1 activity in our mouse model was confirmed at the whole tissue level in non-infarcted hearts; however, we have not evaluated GLO1 activity in either infarcted hearts or at the cellular level. The *hGlo1* transgene is under the control of the preproendothelin-1 promoter, and during MI, elevated preproendothelin-1 mRNA expression has been reported in salvaged cardiomyocytes, endothelial cells, vascular smooth muscle cells, and inflammatory cells within the fibrotic tissue [39]. Also, we have confirmed GLO1 transgene expression in bone marrow cells [42], which are recruited to the myocardium after injury; therefore, it is likely that GLO1 is over-expressed in several cell types in the infarcted hearts of GLO1 mice. Another consideration is that, given the numerous intra- and extra-cellular targets for MG glycation, several mechanisms likely contribute to its detrimental effects post-MI. Although we identified ECM glycation as a possible mechanism, the modification of intracellular signaling cannot be excluded [28]. One likely signaling pathway negatively affected by MG in the post-MI heart is the hypoxia-inducible factor-1α pathway. MG inhibits hypoxia-inducible factor-1α activity leading to decreased transcription of its targets genes (e.g. vascular endothelial growth factor, stromal cell-derived factor-1 and erythropoietin) and reduced angiogenesis [5, 6, 38]. Thus, in the present study, GLO1 over-expression may have increased the production of such growth factors by preventing MG interference on hypoxia-inducible factor-1α activity. Identifying the various MG targets and distinguishing between primary and secondary effects of MG post-MI presents a future research opportunity. Regardless, our study highlights that targeting MG-AGE production post-MI offers cardioprotective benefits.

In summary, this study establishes a possible causative role for MG in LV remodeling and deterioration of cardiac function post-MI. Given that MG and its AGEs are prevalent in diabetes, smoking, and the western diet, and have now been shown to be deleterious in non-diabetic MI, this report highlights a need to reconsider the attention given to MG-AGEs in cardiovascular disease and the development of its therapies.

Acknowledgements The authors would like to thank Rick Seymour and Suzanne Crowe (University of Ottawa Heart Institute) for technical support. This work was supported by operating Grants from the Heart and Stroke Foundation of Canada (HSFC; GIA-000225), and the Canadian Institutes of Health Research (CIHR; FRN 125678). Nick Blackburn was supported by a University of Ottawa Faculty of Medicine Endowed Fund for Cardiac Research and the UOHI Foundation; Branka Vulesevic by a Canadian Graduate Scholarship from the CIHR; and Brian McNeill by a Research Fellowship Award from the HSFC.

Compliance with ethical standards

Conflict of interest PJB has a financial interest in PreventAGE Healthcare, where the mass spectrometry of MG-AGEs was performed. The authors declare no other potential conflicts of interest.

References

1. Ahmed N, Argirov OK, Minhas HS, Cordeiro CA, Thornalley PJ (2002) Assay of advanced glycation endproducts (AGEs): surveying AGEs by chromatographic assay with derivatization by 6-aminoquinolyl-*N*-hydroxysuccinimidyl-carbamate and application to nepsilon-carboxymethyl-lysine- and nepsilon-(1-carboxyethyl)lysine-modified albumin. Biochem J 364:1–14. doi:10.1042/bj3640001
2. Aleshin A, Ananthakrishnan R, Li Q, Rosario R, Lu Y, Qu W, Song F, Bakr S, Szabolcs M, D'Agati V, Liu R, Homma S, Schmidt AM, Yan SF, Ramasamy R (2008) RAGE modulates myocardial injury consequent to LAD infarction via impact on JNK and STAT signaling in a murine model. Am J Physiol Heart Circ Physiol 294:H1823–H1832. doi:10.1152/ajpheart.01210.2007
3. Artym VV, Matsumoto K (2010) Imaging cells in three-dimensional collagen matrix. Curr Protoc Cell Biol 18:11–20. doi:10.1002/0471143030.cb1018s48 **(Chapter 10:Unit 10)**
4. Beisswenger PJ, Howell SK, Russell G, Miller ME, Rich SS, Mauer M (2014) Detection of diabetic nephropathy from advanced glycation endproducts (AGEs) differs in plasma and urine, and is dependent on the method of preparation. Amino Acids 46:311–319. doi:10.1007/s00726-013-1533-x
5. Bento CF, Fernandes R, Ramalho J, Marques C, Shang F, Taylor A, Pereira P (2010) The chaperone-dependent ubiquitin ligase CHIP targets HIF-1alpha for degradation in the presence of methylglyoxal. PLoS One 5:e15062. doi:10.1371/journal.pone.0015062
6. Ceradini DJ, Yao D, Grogan RH, Callaghan MJ, Edelstein D, Brownlee M, Gurtner GC (2008) Decreasing intracellular superoxide corrects defective ischemia-induced new vessel formation in diabetic mice. J Biol Chem 283:10930–10938. doi:10.1074/jbc.M707451200
7. Condorelli G, Roncarati R, Ross J Jr, Pisani A, Stassi G, Todaro M, Trocha S, Drusco A, Gu Y, Russo MA, Frati G, Jones SP, Lefer DJ, Napoli C, Croce CM (2001) Heart-targeted overexpression of caspase3 in mice increases infarct size and depresses cardiac function. Proc Natl Acad Sci USA 98:9977–9982. doi:10.1073/pnas.161120198

8. Discher DE, Mooney DJ, Zandstra PW (2009) Growth factors, matrices, and forces combine and control stem cells. Science 324:1673–1677. doi:10.1126/science.1171643
9. Dobler D, Ahmed N, Song L, Eboigbodin KE, Thornalley PJ (2006) Increased dicarbonyl metabolism in endothelial cells in hyperglycemia induces anoikis and impairs angiogenesis by RGD and GFOGER motif modification. Diabetes 55:1961–1969. doi:10.2337/db05-1634
10. Fadini GP, Losordo D, Dimmeler S (2012) Critical reevaluation of endothelial progenitor cell phenotypes for therapeutic and diagnostic use. Circ Res 110:624–637. doi:10.1161/CIRCRESAHA.111.243386
11. Fazel S, Cimini M, Chen L, Li S, Angoulvant D, Fedak P, Verma S, Weisel RD, Keating A, Li RK (2006) Cardioprotective c-kit^{+} cells are from the bone marrow and regulate the myocardial balance of angiogenic cytokines. J Clin Investig 116:1865–1877. doi:10.1172/JCI27019
12. Francis-Sedlak ME, Moya ML, Huang JJ, Lucas SA, Chandrasekharan N, Larson JC, Cheng MH, Brey EM (2010) Collagen glycation alters neovascularization in vitro and in vivo. Microvasc Res 80:3–9. doi:10.1016/j.mvr.2009.12.005
13. Geoffrion M, Du X, Irshad Z, Vanderhyden BC, Courville K, Sui G, D'Agati VD, Ott-Braschi S, Rabbani N, Thornalley PJ, Brownlee M, Milne RW (2014) Differential effects of glyoxalase 1 overexpression on diabetic atherosclerosis and renal dysfunction in streptozotocin-treated, apolipoprotein E-deficient mice. Physiol Rep. doi:10.14814/phy2.12043
14. Giacco F, Brownlee M (2010) Oxidative stress and diabetic complications. Circ Res 107:1058–1070. doi:10.1161/CIRCRESAHA.110.223545
15. Giacco F, Du X, D'Agati VD, Milne R, Sui G, Geoffrion M, Brownlee M (2014) Knockdown of glyoxalase 1 mimics diabetic nephropathy in nondiabetic mice. Diabetes 63:291–299. doi:10.2337/db13-0316
16. Hanssen NM, Wouters K, Huijberts MS, Gijbels MJ, Sluimer JC, Scheijen JL, Heeneman S, Biessen EA, Daemen MJ, Brownlee M, de Kleijn DP, Stehouwer CD, Pasterkamp G, Schalkwijk CG (2014) Higher levels of advanced glycation endproducts in human carotid atherosclerotic plaques are associated with a rupture-prone phenotype. Eur Heart J 35:1137–1146. doi:10.1093/eurheartj/eht402
17. Harats D, Kurihara H, Belloni P, Oakley H, Ziober A, Ackley D, Cain G, Kurihara Y, Lawn R, Sigal E (1995) Targeting gene expression to the vascular wall in transgenic mice using the murine preproendothelin-1 promoter. J Clin Investig 95:1335–1344. doi:10.1172/JCI117784
18. Hartog JW, Voors AA, Bakker SJ, Smit AJ, van Veldhuisen DJ (2007) Advanced glycation end-products (AGEs) and heart failure: pathophysiology and clinical implications. Eur J Heart Fail 9:1146–1155. doi:10.1016/j.ejheart.2007.09.009
19. Hartog JW, Voors AA, Schalkwijk CG, Scheijen J, Smilde TD, Damman K, Bakker SJ, Smit AJ, van Veldhuisen DJ (2007) Clinical and prognostic value of advanced glycation end-products in chronic heart failure. Eur Heart J 28:2879–2885. doi:10.1093/eurheartj/ehm486
20. Heusch G, Libby P, Gersh B, Yellon D, Böhm M, Lopaschuk G, Opie L (2014) Cardiovascular remodelling in coronary artery disease and heart failure. Lancet 383:1933–1943. doi:10.1016/S0140-6736(14)60107-0
21. Heusch G, Rassaf T (2016) Time to give up on cardioprotection? A critical appraisal of clinical studies on ischemic pre-, post-, and remote conditioning. Circ Res 119:676–695. doi:10.1161/CIRCRESAHA.116.308736
22. Kalra BS, Roy V (2012) Efficacy of metabolic modulators in ischemic heart disease: an overview. J Clin Pharmacol 52:292–305. doi:10.1177/0091270010396042
23. Kang PM, Izumo S (2003) Apoptosis in heart: basic mechanisms and implications in cardiovascular diseases. Trends Mol Med 9:177–182. doi:10.1016/s1471-4914(03)00025-x
24. Kemp CD, Conte JV (2012) The pathophysiology of heart failure. Cardiovasc Pathol 21:365–371. doi:10.1016/j.carpath.2011.11.007
25. Kuraitis D, Hou C, Zhang Y, Vulesevic B, Sofrenovic T, McKee D, Sharif Z, Ruel M, Suuronen EJ (2011) Ex vivo generation of a highly potent population of circulating angiogenic cells using a collagen matrix. J Mol Cell Cardiol 51:187–197. doi:10.1016/j.yjmcc.2011.04.011
26. Kuzuya M, Satake S, Ai S, Asai T, Kanda S, Ramos MA, Miura H, Ueda M, Iguchi A (1998) Inhibition of angiogenesis on glycated collagen lattices. Diabetologia 41:491–499. doi:10.1007/s001250050937
27. Li SY, Sigmon VK, Babcock SA, Ren J (2007) Advanced glycation endproduct induces ROS accumulation, apoptosis, MAP kinase activation and nuclear O-GlcNAcylation in human cardiac myocytes. Life Sci 80:1051–1056. doi:10.1016/j.lfs.2006.11.035
28. Maessen DE, Stehouwer CD, Schalkwijk CG (2015) The role of methylglyoxal and the glyoxalase system in diabetes and other age-related diseases. Clin Sci 128:839–861. doi:10.1042/CS20140683
29. Masoud WG, Ussher JR, Wang W, Jaswal JS, Wagg CS, Dyck JR, Lygate CA, Neubauer S, Clanachan AS, Lopaschuk GD (2014) Failing mouse hearts utilize energy inefficiently and benefit from improved coupling of glycolysis and glucose oxidation. Cardiovasc Res 101:30–38. doi:10.1093/cvr/cvt216
30. Molgat AS, Tilokee EL, Rafatian G, Vulesevic B, Ruel M, Milne R, Suuronen EJ, Davis DR (2014) Hyperglycemia inhibits cardiac stem cell-mediated cardiac repair and angiogenic capacity. Circulation 130:S70–S76. doi:10.1161/CIRCULATIONAHA.113.007908
31. Mulder DJ, van Haelst PL, Graaff R, Gans RO, Zijlstra F, Smit AJ (2009) Skin autofluorescence is elevated in acute myocardial infarction and is associated with the one-year incidence of major adverse cardiac events. Neth Heart J 17:162–168. doi:10.1007/BF03086239
32. Ohtsuka M, Takano H, Zou Y, Toko H, Akazawa H, Qin Y, Suzuki M, Hasegawa H, Nakaya H, Komuro I (2004) Cytokine therapy prevents left ventricular remodeling and dysfunction after myocardial infarction through neovascularization. FASEB J 18:851–853. doi:10.1096/fj.03-0637fje
33. Rabbani N, Thornalley PJ (2014) Measurement of methylglyoxal by stable isotopic dilution analysis LC-MS/MS with corroborative prediction in physiological samples. Nat Protoc 9:1969–1979. doi:10.1038/nprot.2014.129
34. Rabbani N, Thornalley PJ (2012) Methylglyoxal, glyoxalase 1 and the dicarbonyl proteome. Amino Acids 42:1133–1142. doi:10.1007/s00726-010-0783-0
35. Rabbani N, Xue M, Thornalley PJ (2016) Methylglyoxal-induced dicarbonyl stress in aging and disease: first steps towards glyoxalase 1-based treatments. Clin Sci 130:1677–1696. doi:10.1042/CS20160025
36. Takagawa J, Zhang Y, Wong ML, Sievers RE, Kapasi NK, Wang Y, Yeghiazarians Y, Lee RJ, Grossman W, Springer ML (2007) Myocardial infarct size measurement in the mouse chronic infarction model: comparison of area- and length-based approaches. J Appl Physiol 102:2104–2111. doi:10.1152/japplphysiol.00033.2007
37. Talior-Volodarsky I, Connelly KA, Arora PD, Gullberg D, McCulloch CA (2012) alpha11 integrin stimulates myofibroblast differentiation in diabetic cardiomyopathy. Cardiovasc Res 96:265–275. doi:10.1093/cvr/cvs259
38. Thangarajah H, Yao D, Chang EI, Shi Y, Jazayeri L, Vial IN, Galiano RD, Du XL, Grogan R, Galvez MG, Januszyk M,

Brownlee M, Gurtner GC (2009) The molecular basis for impaired hypoxia-induced VEGF expression in diabetic tissues. Proc Natl Acad Sci USA 106:13505–13510. doi:10.1073/pnas.0906670106

39. Tonnessen T, Lunde PK, Giaid A, Sejersted OM, Christensen G (1998) Pulmonary and cardiac expression of preproendothelin-1 mRNA are increased in heart failure after myocardial infarction in rats. Localization of preproendothelin-1 mRNA and endothelin peptide. Cardiovasc Res 39:633–643. doi:10.1016/S0008-6363(98)00156-4
40. Venkatraman J, Aggarwal K, Balaram P (2001) Helical peptide models for protein glycation: proximity effects in catalysis of the Amadori rearrangement. Chem Biol 8:611–625. doi:10.1016/S1074-5521(01)00036-9
41. Verzijl N, DeGroot J, Thorpe SR, Bank RA, Shaw JN, Lyons TJ, Bijlsma JW, Lafeber FP, Baynes JW, TeKoppele JM (2000) Effect of collagen turnover on the accumulation of advanced glycation end products. J Biol Chem 275:39027–39031. doi:10.1074/jbc.M006700200
42. Vulesevic B, McNeill B, Geoffrion M, Kuraitis D, McBane JE, Lochhead M, Vanderhyden BC, Korbutt GS, Milne RW, Suuronen EJ (2014) Glyoxalase-1 overexpression in bone marrow cells reverses defective neovascularization in STZ-induced diabetic mice. Cardiovasc Res 101:306–316. doi:10.1093/cvr/cvt259
43. Vulesevic B, McNeill B, Giacco F, Maeda K, Blackburn NJ, Brownlee M, Milne RW, Suuronen EJ (2016) Methylglyoxal-induced endothelial cell loss and inflammation contribute to the development of diabetic cardiomyopathy. Diabetes 65:1699–1713. doi:10.2337/db15-0568
44. Vulesevic B, Milne RW, Suuronen EJ (2014) Reducing methylglyoxal as a therapeutic target for diabetic heart disease. Biochem Soc Trans 42:523–527. doi:10.1042/BST20130254
45. Wencker D, Chandra M, Nguyen K, Miao W, Garantziotis S, Factor SM, Shirani J, Armstrong RC, Kitsis RN (2003) A mechanistic role for cardiac myocyte apoptosis in heart failure. J Clin Investig 111:1497–1504. doi:10.1172/jci200317664
46. Yao D, Brownlee M (2010) Hyperglycemia-induced reactive oxygen species increase expression of the receptor for advanced glycation end products (RAGE) and RAGE ligands. Diabetes 59:249–255. doi:10.2337/db09-0801
47. Yuen A, Laschinger C, Talior I, Lee W, Chan M, Birek J, Young EW, Sivagurunathan K, Won E, Simmons CA, McCulloch CA (2010) Methylglyoxal-modified collagen promotes myofibroblast differentiation. Matrix Biol 29:537–548. doi:10.1016/j.matbio.2010.04.004